Appl. Phys. B 70, 683–688 (2000) / Digital Object Identifier (DOI) 10.1007/s003400000273

Applied Physics B
Lasers
and Optics

Adiabatic focusing of cold atoms in a blue-detuned laser standing wave

L. Khaykovich, N. Davidson

Department of Physics of Complex Systems, Weizmann Institute of Science, Rehovot 76100, Israel

Received: 1 October 1999/Revised version: 13 December 1999/Published online: 5 April 2000 – © Springer-Verlag 2000

Abstract. Adiabatic focusing of cold atoms in a blue-detuned laser standing wave is analyzed. It is shown that using repulsive light forces that push atoms towards dark regions and thus minimizes heating, cold atoms can be adiabatically compressed by more than an order of magnitude to yield background-free sub-10-nm (rms) spots. The optimal parameters for the atomic lens and the maximal compression ratio are predicted using an analytic model and found to be in agreement with the exact results of our Monte Carlo simulations. A combined adiabatic-coherent scheme is proposed and shown to yield 8.8 nm spot size even for a thermal atomic beam.

PACS: 03.75.Be; 42.50.Vk; 32.80.Pj; 42.82.Cr; 85.40.Ux

Atomic lithography, a technique of direct deposition of neutral atoms using nearly conservative light–atom interactions, has been intensively studied in recent years. In particular, sub-100-nm features were demonstrated for sodium [1], chromium [2, 3] and aluminium [4] atoms. In a different approach, cesium [5, 6] and metastable argon and helium atoms [7, 8] have been used in resist-based processes. In all these experiments, a thermal atomic beam was cooled transversely and then focused by the dipole potential of a standing-wave laser light into periodic structures. The standing wave provides what is known as coherent focusing, where the atoms complete a quarter oscillation period and the focus is located within the laser light intensity. This coherent focusing suffers from a wide spectrum of aberrations that have been addressed theoretically and experimentally by number of authors [9]. These aberrations broaden the atomic deposited pattern above the "diffraction limited" resolution and also produce a significant background of atoms.

In parallel, laser cooling techniques have made significant progress during this time and new and bright sources of cold atoms have been developed [10, 11]. However, using longitudinally slow atoms for atomic lithography has yet to be reported. Replacing the thermal atomic beam with a cold atomic source can reduce some of the main aberrations of the atomic lenses, and also result in substantially longer interaction time between the atoms and the focusing dipole potential. This opens the possibility to exploit adiabatic mechanisms for efficient focusing techniques. Adiabatic focusing is expected to be extremely robust as compared to coherent focusing. In particular, it is expected to be nearly insensitive to the exact shape of the potential (spherical aberration), the longitudinal velocity spread (chromatic aberration), variations of the dipole potential among atoms in different internal states and deviations of the deposited surface from the focal point [2, 12]. On the other hand, it is more sensitive to transverse velocity distribution, to heating of the atoms by the focussing laser and to the "diffraction limited" resolution, which is the size of the ground state wavefunction of the final potential. Channeling of atoms to dipole-potential minima in a standing wave has been observed for a thermal atomic beam [13], but the short interaction time and high transverse temperatures there resulted in relatively poor localization.

A laser standing wave was also used both to de-excite metastable argon atoms to an inert ground state and to confine the remaining metastable atoms in an optical potential to generate sub-0.1 μm atomic lithography [14]. Finally, the inverse process to adiabatic focusing, namely adiabatic cooling, has also been demonstrated [15].

In this paper we analyze adiabatic focusing of atoms by a laser standing wave. We present an analytical model that describes the lens aberration in this regime and use it for global optimization of the lens parameters. We show that with repulsive light forces, which push atoms towards dark regions and thus minimize heating by the light field, cold atoms can be compressed adiabatically by more than an order of magnitude with readily accessible laser powers. Furthermore, nearly background-free structures can be obtained. The optimal lens parameters, as well as the compression ratios are in good agreement with the exact results of our Monte Carlo simulations. Finally, we show that by combining adiabatic focusing with coherent focusing a further improvement of the compression ratio is obtained. In this configuration, the adiabatic focusing acts as a preparation stage that brings the atoms closer to the potential minima, where aberrations are small.

All our analysis is performed on rubidium atoms, which we plan to use for our experiments. However, a simple scaling law for most of our results enables one to apply them to other atoms such as cesium, aluminium and chromium.

1 Analytic approach

We consider a one dimensional (1-D) atomic lens configuration which is based on interaction of longitudinally and transversely cold atoms with a 1-D linearly polarized standing wave, oriented perpendicular to the atomic beam that propagates in the z direction, as shown in Fig. 1a. The intensity distribution of the standing wave is:

$$I(x, z, y \simeq 0) = 4\frac{2P}{\pi w_y w_z} \mathrm{e}^{-\frac{z^2}{2w_z^2}} \sin^2(kx), \tag{1}$$

where P is the laser power, w_y and w_z are laser beam waists in the y and z directions respectively, and $k = 2\pi/\lambda$ is the wave number. While w_z will be determined uniquely by our model through the limitation of the minimal interaction time, w_y is selected by practical considerations, e.g. the substrate

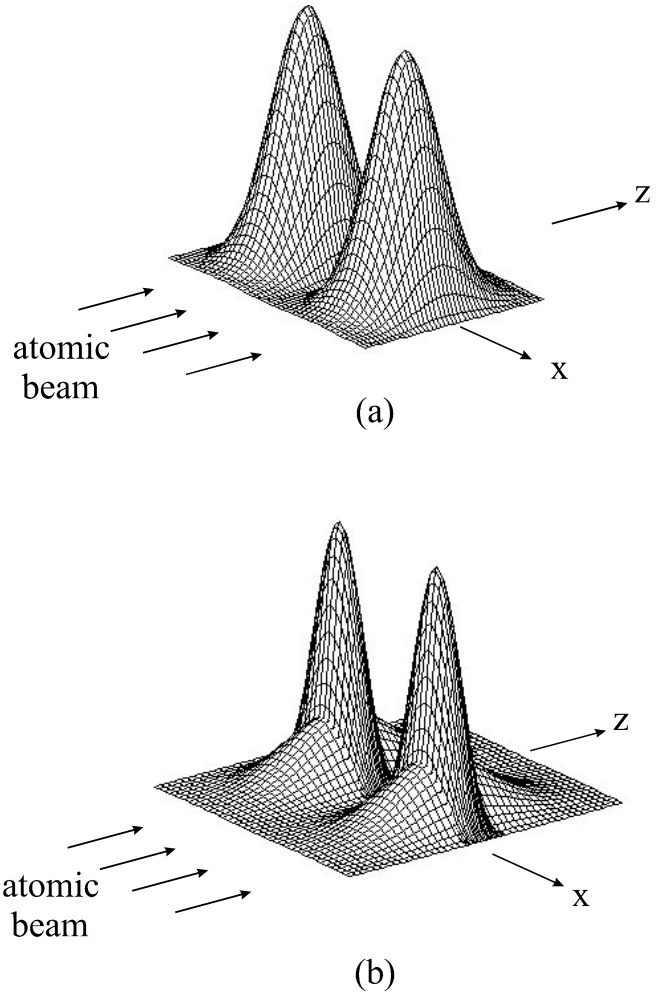

Fig. 1a,b. Schematic diagram of the experimental arrangement and dipole potential in one period of the standing wave: **a** adiabatic lens, **b** combined adiabatic and coherent lenses

area needed to be deposited in parallel [16]. The standing wave produces gradients of the electric field in the x direction with periodicity of $\lambda/2$. Atoms are attracted to the light intensity maximum for red-detuned light and are repelled from the high intensity region for blue-detuned light. Our analysis concentrates on the repulsive regime for reasons that are addressed below.

The long interaction time that is necessarily obtained for cold atoms has two novel aspects for the focusing process. First, this time becomes longer than the oscillation time of atoms around the nodes of the standing wave. Hence, atoms will cross the potential minimum several times before they reach the focus region. Since the potential strength increases with penetration depth, atoms that are slow enough to follow potential changes adiabatically will compress toward the nodes of the standing wave.

Second, the number of spontaneously emitted photons per atom grows linearly with the interaction time and therefore may not be neglected as is often done for thermal atomic beams. Two heating mechanisms relate to spontaneously emitted photons: the first caused by their randomly directed momentum kick and the second caused by dipole force fluctuations. For blue-detuned light, atoms compress adiabatically to the nodes of the standing wave, where the probability of spontaneous events is significantly suppressed. This enables the use of smaller detunings for the focusing laser and, as a result, stronger potentials and higher compression ratios. Furthermore, for blue-detuned intense standing wave sisyphus cooling may provide dissipation and further reduce diffusive heating as compared to the red-detubed case. However, this effect is not expected to be efficient because the transverse kinetic energy of atoms is much smaller than the potential depth during most of the adiabatic compression [17]. To obtain an upper limit for the spot size we shall therefore neglect it altogether.

To develop an analytic model for adiabatic focusing we first determine the minimal interaction time that still satisfies the adiabatic condition. This time is estimated to be the longest oscillation time ($T_{\mathrm{osc}}^{\max}$), calculated for the smallest potential that is significant for the atoms, namely a potential equal to their initial transverse kinetic energy $U_1 = k_{\mathrm{B}} T_{\perp}$. Using a parabolic approximation for the small amplitude oscillation times yields

$$t_{\mathrm{int}} = T_{\mathrm{osc}}^{\max} = \frac{1}{\nu_{\mathrm{r}}}\sqrt{\frac{U_{\mathrm{r}}}{2U_1}}, \tag{2}$$

where $U_{\mathrm{r}} = (\hbar k)^2/m$ and $\nu_{\mathrm{r}} = U_{\mathrm{r}}/h$ are the recoil energy and recoil frequency, respectively. If $U_1 < \frac{18}{\pi^4} U_{\mathrm{r}}$, the latter should be used instead. This yields the "diffraction limited" spot size, which is in this case the size of the ground state of the maximal potential $(\hbar T_{\mathrm{osc}}^{\min}/(4\pi m))^{1/2}$. Our exact numerical calculations (described below) show that when (2) is fulfilled, the spot size of adiabatic focussing is only 25% larger than for an "infinite" interaction time, verifying the validity of our estimation. The choice of interaction time defines the w_z that ensures adiabaticity as:

$$w_z = v_z T_{\mathrm{osc}}^{\max} = \frac{v_z}{\nu_{\mathrm{r}}}\sqrt{\frac{U_{\mathrm{r}}}{2U_1}}, \tag{3}$$

where v_z is the most probable longitudinal velocity of atoms. This value for w_z is also expected to be optimal for adiabatic compression since for larger w_z the maximal dipole potential, which is applied to atoms, decreases.

Next, the detuning of the laser from the atomic resonance (δ) is optimized to maximize the (maximal) dipole potential. For a two-level atom the dipole potential is [18]:

$$U = \frac{\hbar\delta}{2}\ln(1+s), \tag{4}$$

where $s = \frac{2\Omega_r^2}{\gamma^2+4\delta^2}$ is the saturation parameter, $\Omega_r = \gamma\sqrt{0.5I/I_s}$ is the Rabi frequency, γ the atomic transition line width, and I_s the saturation intensity. For $\delta \gg \gamma$ this potential optimizes for

$$\delta_{opt} \simeq 0.35\Omega_r, \tag{5}$$

and is expressed as: $U(\delta = \delta_{opt}) \simeq 0.28\hbar\gamma(I/I_s)^{1/2}$. Substituting (3) and (1) for $I(x = \lambda/4,\ y = z = 0)$ yields the maximum dipole potential as:

$$U_{max} \simeq 0.54\hbar\gamma\left(\frac{1}{I_s}\frac{P}{\pi w_y}\frac{\gamma}{v_z}\right)^{1/2}\left(\frac{\nu_r}{\gamma}\right)^{1/2}\left(\frac{U_1}{U_r}\right)^{1/4}. \tag{6}$$

To calculate the adiabatic compression ratio C (the ratio between initial rms size of the atomic distribution and the final rms spot size) we first neglect all diffusive heating. The compression is then limited only by the initial transverse kinetic energy as:

$$C = c\left(\frac{U_{max}}{U_1}\right)^{1/4} \simeq c\cdot 0.86\left(\frac{1}{I_s}\frac{P}{\pi w_y}\frac{\gamma}{v_z}\right)^{1/8}\left(\frac{\gamma}{\nu_r}\right)^{1/8}\left(\frac{U_r}{U_1}\right)^{3/16}, \tag{7}$$

where $c \simeq 0.75$ corrects for the partial failure of adiabaticity due to the finite interaction time. For an initial atomic distribution which is uniform over the lens size $\lambda/2$ with an initial rms size of $x_{rms}^{init} = \lambda/(2\sqrt{12})$ the final rms spot size (at $z \simeq 0$) is finally given as

$$x_{rms}^{final} = \frac{x_{rms}^{init}}{C} \simeq 0.21\lambda\left(I_s\frac{\nu_r}{\gamma}\frac{w_y}{P}\frac{v_z}{\gamma}\right)^{1/8}\left(\frac{U_1}{U_r}\right)^{3/16}. \tag{8}$$

As expected, better focusing is obtained for atoms with smaller transverse kinetic energy U_1, smaller longitudinal velocity v_z and for focusing laser beam with higher power P and smaller waist w_y. However, the latter three appear with a 1/8 power law and hence affect the spot size very weakly.

To justify the neglect of spontaneous scattering, we now show that the heating owing to momentum diffusion is smaller than the adiabatic heating due to the compression. The momentum diffusion coefficient for a two-level atom, subjected to standing wave potential, is a sum of vacuum (D_{vac}) and dipole (D_{dip}) diffusion coefficients [18]:

$$\begin{aligned} D(x,z) &= D_{vac} + D_{dip}^{(1)} + D_{dip}^{(2)} + D_{dip}^{(3)} + D_{dip}^{(4)} \\ &= (\hbar k)^2\frac{\gamma}{4}\frac{s(x,z)}{1+s(x,z)} + (\hbar\alpha(x,z))^2\frac{s(x,z)}{(1+s(x,z))^3} \\ &\quad\times\left(1 + \frac{-4\delta^2+3\gamma^2}{4\delta^2+\gamma^2}s(x,z) \right. \\ &\quad\left. +3s^2(x,z) + \frac{4\delta^2+\gamma^2}{\gamma^2}s^3(x,z)\right), \end{aligned} \tag{9}$$

where $\alpha(x,z) = \frac{\nabla\Omega_r(x,z)}{\Omega_r(x,z)}$. Averaging over fast oscillations in the x direction, yields $\overline{D}(z) = D(x_{rms}(z))$, where $x_{rms}(z) = \left(\frac{U(z)}{U_1}\right)^{1/4}x_{rms}^{init}$ according to the adiabatic law. For $s \gg 1$, the main contribution to the dipole diffusion coefficient is from the last term ($D_{dip}^{(4)}$) in (9) which increases linearly with s. However, this term vanishes at nodes and antinodes of the standing wave, as shown in Fig. 2, where it is presented together the first dipole term and the vacuum term. Moreover, $D_{dip}^{(4)}$ has an x^6 dependence around nodes, while near antinodes it has a much steeper dependence $\propto x^2$. For blue detuning, atoms are adiabatically compressed toward nodes

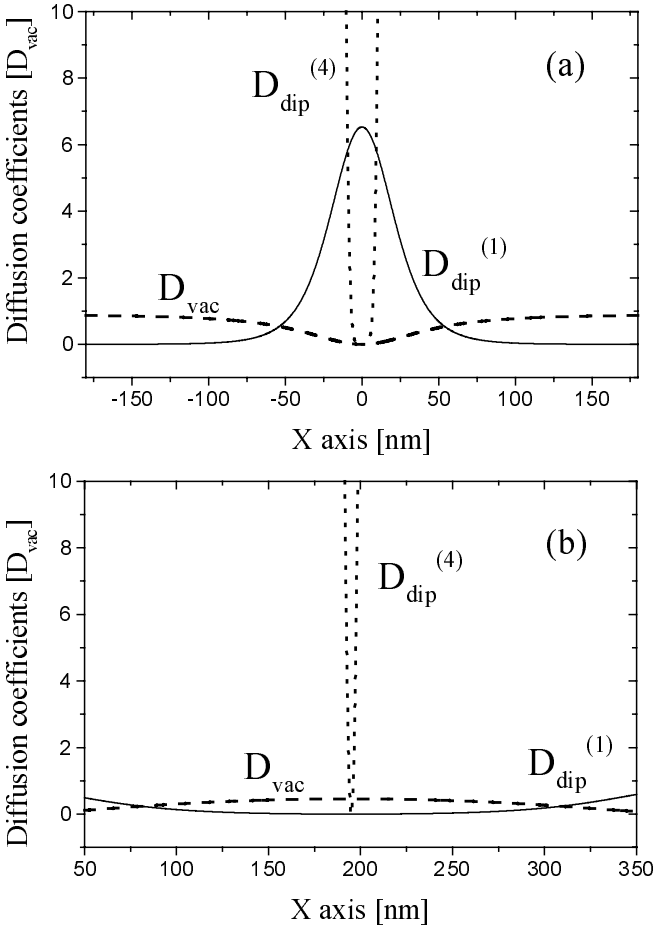

Fig. 2a,b. Spatial dependence of the vacuum (*dashed line*) as well as first (*solid line*) and last (*dotted line*) terms of the dipole diffusion coefficients in units of maximal D_{vac} for $P/w_y = 1\,\mathrm{W/cm}$, $w_z = 25\,\mu\mathrm{m}$ and $\delta = 70\gamma$ **a** near node (for blue-detuned standing wave); **b** near antinode (for red-detuned standing wave)

of the standing wave and hence feel much smaller diffusion heating than for red detuning.

Quantitatively, the rms momentum increase due to diffusion is obtained by integration of the various diffusion coefficients over the interaction time ($t_{\rm int}$) : $p^2_{\rm rms} = \int \overline{D}(z(t))\,{\rm d}t$. Substituting expressions of different diffusion coefficients and their x dependence and assuming paraxial motion near the node yields the rms momentum increase due to $D_{\rm vac}$, $D^{(1)}_{\rm dip}$, and $D^{(4)}_{\rm dip}$ as:

$$(p^{\rm vac}_{\rm rms})^2 = \frac{1}{4}(\hbar k)^2 (k x^{\rm rms}_{\rm init}) \frac{\gamma}{4} \frac{(U_1 U_{\rm max})^{1/2}}{\hbar\delta} \frac{t_{\rm int}}{2}, \tag{10}$$

$$(p^{\rm dip(1)}_{\rm rms})^2 = \frac{1}{2}(\hbar k)^2 \frac{\gamma}{4} \frac{U_{\rm max}}{\hbar\delta} t_{\rm int}, \tag{11}$$

$$(p^{\rm dip(4)}_{\rm rms})^2 = \frac{1}{16}(\hbar k)^2 \frac{1}{8} (k x^{\rm rms}_{\rm init})^6 \frac{\gamma}{4} \frac{U_1^{3/2} U_{\rm max}^{5/2}}{(\hbar\delta)^4} t_{\rm int}. \tag{12}$$

The $D^{(2)}_{\rm dip}$ and $D^{(3)}_{\rm dip}$ provide negligible heating.

The momentum increase due to different diffusion coefficients, normalized to the momentum increase due to adiabatic heating $(p^{\rm add}_{\rm rms})^2 = 2m(U_1 U_{\rm max})^{1/2}$ is shown in Fig. 3a as a function of the atomic velocity for $P/w_y = 1\,{\rm W/cm}$ (w_z and δ are determined for each velocity to their optimal values given by (3) and (5)). For the whole range of atomic velocities, the diffusion heating is smaller than the adiabatic heating, and can indeed be neglected. Therefore, (8) is valid for adiabatic focusing by the blue-detuned standing wave for most practical cases. For the red-detuned case with the same parameters, diffusive heating cannot be neglected as compared to the adiabatic heating. Hence, the optimal detuning increases and the amount of compression decreases compared to the blue-detuned case [19].

The analytically predicted compression ratio as a function of v_z is shown in Fig. 3b, for the parameters $P/w_y = 1\,{\rm W/cm}$ and $U_1 = 9U_{\rm r}$. For small velocities the predicted compression ratio is very large, because a small laser beam waist produces a strong dipole potential. For higher velocity, a wider beam waist is needed to maintain adiabatic conditions, so the dipole potential decreases and the final spot size increases.

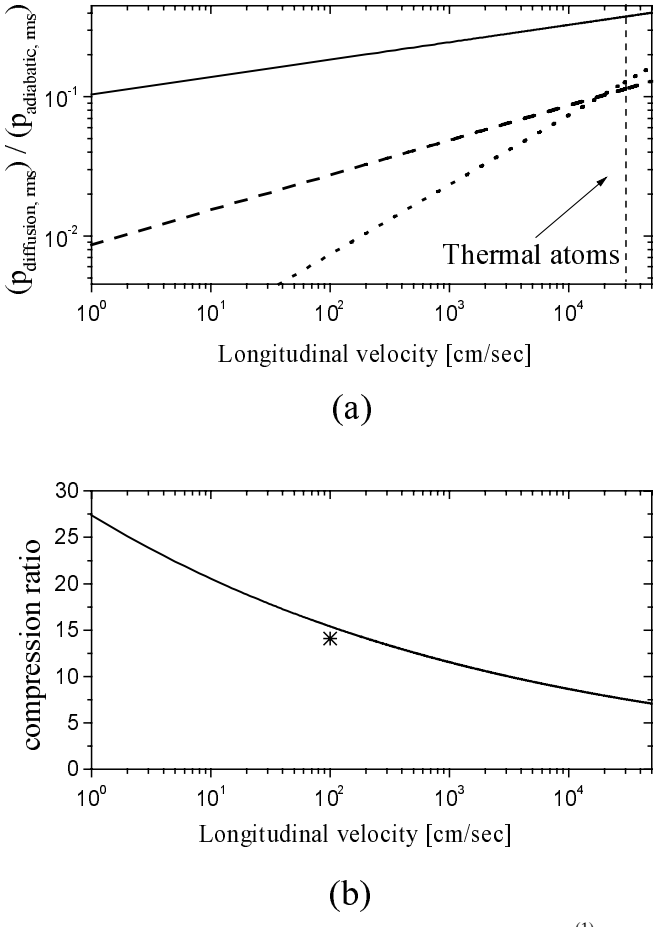

Fig. 3. a The momentum increase due to $D_{\rm vac}$ (*dashed line*), $D^{(1)}_{\rm dip}$ (*solid line*) and $D^{(1)}_{\rm dip}$ (*dotted line*) diffusion coefficients, normalized to the momentum increase due to adiabatic heating, as a function of the longitudinal velocity of the atomic beam; **b** the analytically predicted compression ratio, where *the star* indicates our exact Monte Carlo simulations

2 Monte Carlo simulations

To verify our analytic predictions, we performed exact Monte Carlo simulations of the adiabatic focusing of atoms with a blue-detuned standing wave. We simulated ^{85}Rb atoms that are pushed from a magneto-optical trap toward the standing wave to reach a desired longitudinal velocity of $v_z = 1\,{\rm m/s}$ while preserving small velocity spreads. A large number of classical trajectories were calculated for different random initial conditions of position, velocity and angle. The longitudinal and transverse rms velocity spreads are $3v_{\rm r}$. Our simulations for 10 times higher temperature showed an increase in the final spot by $\sim 50\%$ in agreement with the analytic predictions of (8). We include in the simulations all effects related to spontaneously scattered photons, by calculating the exact diffusion coefficient at each time step and then adding a randomly distributed momentum kick, with the $p_{\rm rms}$ value corresponding to the diffusion coefficient. We also assumed that atoms in the incoming atomic beam are distributed uniformly among the different magnetic sublevel (m-states) and accounted for their different interaction strengths with the laser light. Each time a spontaneous emission occurred in the simulations, the redistribution in m-states was randomly selected according to the correct Clebsch–Gordan coefficients. We verified that focusing is largely insensitive to the m-state distribution, as expected for an adiabatic process.

We chose the power of the laser to be $P = 1\,{\rm W}$ and fixed $w_y = 1\,{\rm cm}$. Our simulations for 10 times smaller P/w_y showed an increase in the final spot by only $\sim 30\%$ in agreement with the analytic predictions of (8). The final rms size of the compressed atoms is shown in Fig. 4 as a function of w_z. As seen, a clear optimized value of $w_z \simeq 25\,\mu{\rm m}$ is obtained. For very small laser beam waists the adiabatic condition is no longer fulfilled, and the lens parameters approach those of a coherent ($T_{\rm osc}/4$) lens. The spot size in this case increases rapidly due to various aberrations and especially the spherical one. Note that the number of atoms that arrived at the central peak still grows toward small waists (second curve in Fig. 4). Growth of the rms size $w_z > 25\,\mu{\rm m}$ is due to the decrease in the dipole potential strength, in agreement with the prediction of (6). Note that the minimal rms spot size of 8 nm is still ~ 2 times larger than the rms size of the ground state of the potential (which is 4.2 nm in this case).

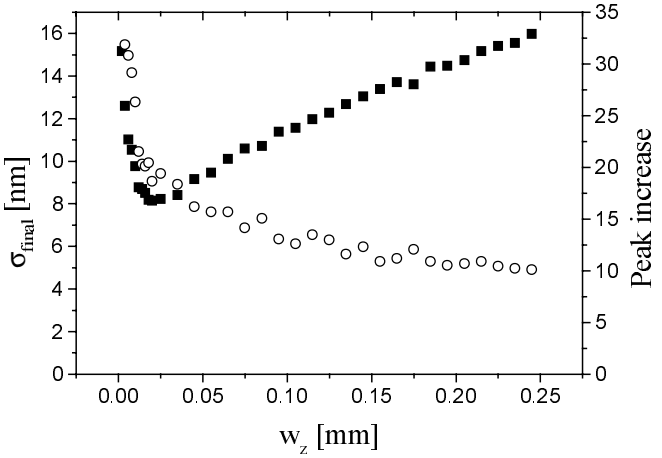

Fig. 4. The final rms size of the compressed atoms (■) and the increase in the peak of the compressed atomic distribution (◯) as a function of w_z for $P/w_y = 1\,\mathrm{W/cm}$, $\delta = 70\gamma$, $v_z = 1\,\mathrm{m/s}$, and $U_1 = 9U_\mathrm{r}$

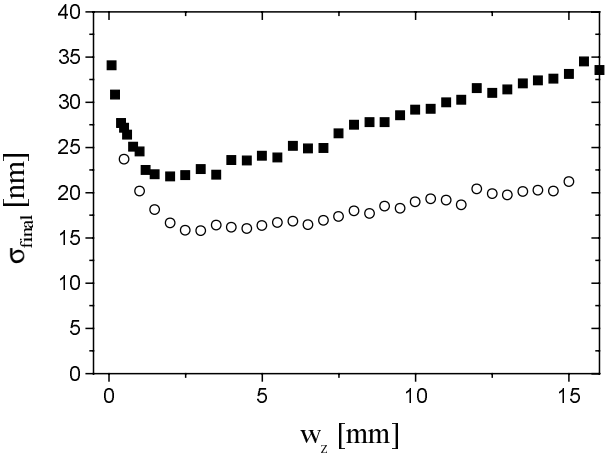

Fig. 5. The final rms size of the compressed thermal atoms for $\delta = 14\gamma$ and $w_y = 1\,\mathrm{cm}$ (■) and for $\delta = 42\gamma$ and $w_y = 1\,\mathrm{mm}$ (◯) as a function of w_z for $v_z = 300\,\mathrm{m/s}$ and $U_1 = 9U_\mathrm{r}$

To verify that our analytically predicted parameters provide global optimization of the adiabatic lens, we simulated the spot size as a function of both laser detuning and laser beam waist, and found a global minimum at $w_z \simeq 25\,\mu\mathrm{m}$ and $\delta \simeq 70\gamma - 150\gamma$ which are close to the analytically predicted parameters ($w_z = 30\,\mu\mathrm{m}$ and $\delta = 115\gamma$). The star on the analytical curve in Fig. 3b shows the compression value calculated from full Monte Carlo simulations, which is in agreement with the analytical one to 10%. Finally, we simulated the adiabatic focusing without any diffusion heating, without longitudinal velocity spread, without *m*-state distribution (using 2-level atoms) and for a pure harmonic potential. We found that all these changes yielded negligible changes to the spot size, as expected.

We also performed Monte Carlo simulations for the red-detuned standing wave. In agreement with our analytical predictions, the optimal detuning was obtained when the heating due to diffusion becomes comparable with the adiabatic heating and was larger than that determined by (5). Therefore, the potential depth decreased for the same laser power and the minimal final spot sizes increased by $\sim 60\%$ as compared to the blue-detuned case.

3 Adiabatic and combined lenses for thermal atoms

The insensitivity of the adiabatic lens to most aberrations can also be useful for thermal atomic beams. However, for thermal atoms to fulfill the adiabatic condition, a very wide waist of the laser beam is needed and hence the strength of the dipole potential becomes much smaller than for slow atoms. We repeated the Monte Carlo simulation for a thermal atomic beam emerging from an oven with a most probable longitudinal velocity of $v_z = 300\,\mathrm{m/s}$, laser cooled to a transverse kinetic energy $U_1 = 9U_\mathrm{r}$ and then focused by a laser standing wave with $P/w_y = 1\,\mathrm{W/cm}$ (and $1\,\mathrm{W/mm}$) and $\delta = 14\gamma$ (and 42γ). The final spot size as a function of w_z is shown in Fig. 5. As seen, the general trend for adiabatic compression of thermal atoms is similar to that of slow atoms, but the optimal w_z is ~ 100 times larger. The agreement of the analytic predictions with the exact results is worse for thermal atoms than for slow ones. In particular the predicted optimal w_z is ~ 2 times larger, the predicted optimal δ is ~ 2 times smaller and the predicted spot size is $\sim 30\%$ smaller than the exact results. We attribute these differences to diffuse heating which cannot be neglected as compared to adiabatic heating, in contrast to the slow atom case. We confirm this conjecture by "switching off" the heating in the Monte Carlo simulations and observed an improved agreement with the analytic model.

To further improve the spot size for thermal atoms, we consider a combination of the adiabatic lens with a coherent ($T_\mathrm{osc}/4$) lens. The purpose of the adiabatic lens here is to place the atoms closer to the potential minimum where it is nearly parabolic and hence suffers from smaller aberrations. Then, the coherent lens, which coincides with the adiabatic lens as shown in Fig. 1b, is applied more efficiently.

The combined adiabatic–coherent scheme was analyzed for the thermal atomic beam using the Monte Carlo simulations. The laser powers are $P_\mathrm{coh} = 0.5\,\mathrm{W}$ and $P_\mathrm{ad} = 0.25\,\mathrm{W}$ and laser beam waists are $w_z^\mathrm{coh} = 30\,\mu\mathrm{m}$ and $w_z^\mathrm{ad} = 3\,\mathrm{mm}$, respectively. In order to simplify the set-up and avoid phase shifts between two lenses we chose the same detuning ($\delta = 70\gamma$) for both lasers [20]. Hence, the adiabatic and coherent lenses can be produced by the same laser. For both beams $w_y = 1\,\mathrm{cm}$. In Figs. 6a and 6b the calculated atomic trajectories near the focus are shown for the coherent and the com-

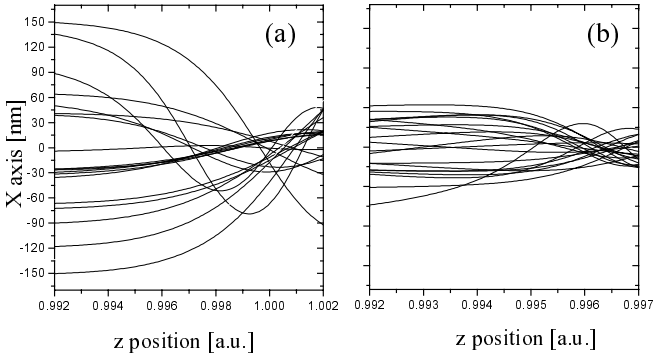

Fig. 6a,b. A number of the calculated atomic trajectories in one period of the standing wave inside a coherent lens for a thermal atomic beam **a** without adiabatic compression and **b** after preliminary compression by an adiabatic lens. The atomic beam parameters are specified in the text

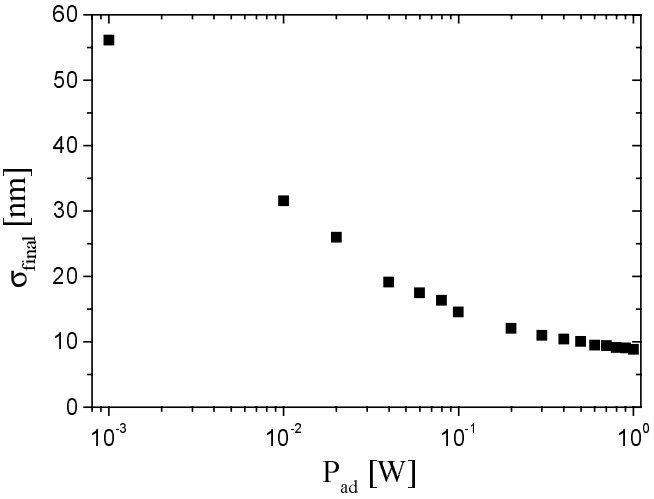

Fig. 7. The final rms spot size for combined adiabatic and coherent lens for thermal atoms ($v_z = 300$ m/s) as a function of the P_{ad} for $w_y = 1$ cm

bined lens, respectively. As seen, the initial atomic beam is compressed by a factor of three after the adiabatic stage. As a result it is compressed by the coherent stage to a smaller spot size than by a coherent lens only, in spite of the extra heating it suffers during the adiabatic stage.

The final rms spot size as a function of P_{ad} is shown in Fig. 7. As seen, the improvement of the combined lens as compared to the coherent lens increases with P_{ad}, and saturates at $P_{ad} \sim 1$ W yielding an rms size of 8.8 nm as compared to 56 nm for the coherent lens only and 22 nm for the adiabatic lens only. This is expected because without aberrations the coherent lens compresses atoms as $(U_{max}/U_1)^{1/2}$, while the adiabatic lens only according to $(U_{max}/U_1)^{1/4}$. Therefore, for large enough P_{ad}, where the aberrations of the coherent lens become negligible, it is the heating due to the adiabatic compression that limits the total focusing performance.

4 Conclusions

In this paper we have presented an analytical and a numerical analysis of the adiabatic focusing of cold atoms in a blue-detuned laser standing wave. The analytical model predicts for given laser power and atomic velocity the optimal beam waist and laser detuning, and the resulting compression ratio. It is also predicts that heating in the standing wave is significantly reduced by channeling of atoms and therefore does not affect the final spot size. The analytical analysis was verified by exact Monte Carlo simulations that include heating effects, m-state distributions, transverse and longitudinal velocity distributions and spherical aberrations. The results show that although adiabatic focusing scales as $U_{max}^{1/4}$ as compared to the coherent one which scales as $U_{max}^{1/2}$, it is dramatically insensitive to most aberrations. Hence, adiabatic focusing of cold atoms by more than an order of magnitude and sub-10-nm rms spot sizes can be obtained over large areas with readily available laser powers. An additional advantage of depositing cold atoms is that, due to the much smaller kinetic energy, surface diffusion may decrease as compared to thermal atoms [12].

We also analyzed the adiabatic focusing for a thermal atomic beam and found it to be considerably worse than for cold atoms. However, a combination of adiabatic and coherent focusing was shown to improve the rms spot size by a factor of ~ 6.5 and ~ 2.5 as compared to purely coherent and purely adiabatic focusing, respectively, and to yield sub-10-nm rms spot sizes even for thermal (but transversely cold) atomic beams.

Finally, our results can be simply scaled for Cr atoms. Using (7) and atomic constants of Cr, the final compression ratio for Cr atoms will by smaller by factor of 2 and the final spot size will be approximately the same as we calculated for ^{85}Rb.

References

1. G. Timp, R.E. Behringer, D.M. Tennant, J.E. Canningham, M. Prentiss, K.K. Breggren: Phys. Rev. Lett. **69**, 1636 (1992)
2. J.J. McClelland, R.E. Scholten, E.C. Palm, R.G. Celotta: Science **262**, 877 (1993)
3. U. Drodofsky, J. Stuhler, B. Brezger, Th. Shulze, M. Drewsen, T. Pfau, J. Mlynek: Microelectron. Eng. **35**, 285 (1997)
4. R.W. McGowan, D.M. Giltner, S.A. Lee: Opt. Lett. **20**, 2535 (1995)
5. M. Kreis, F. Lison, D. Haubrich, S. Nowak, T. Pfau, D. Meschede: Appl. Phys. B **63**, 649 (1996)
6. K.K. Berggren, R. Younkin, E. Cheung, M. Prentiss, A. Black, G.M. Whitesides, D.C. Ralph, C.T. Black, M. Tinkham: Adv. Mater. **9**, 52 (1997)
7. K.K. Berggren, A. Bard, J.L. Wilbur, J.D. Gillaspy, A.G. Helg, J.J. McClleland, S.L. Rolston, W.D. Phillips, M. Prentiss, G.M. Whitesides: Science **269**, 1255 (1995)
8. S. Nowak, T. Pfau, J. Mlynek: Appl. Phys. B **63**, 203 (1996)
9. V.I. Balykin, V.S. Letokhov: Opt. Commun. **64**, 151 (1987); G.M. Gallatin, P. Gould: *ibid*. **8**, 502 (1991); J.J. McClelland, M.R. Scheinfein: *ibid*. **8**, 1974 (1991); K.K. Berggren, M. Prentiss, G.L. Timp, R.E. Behringer: *ibid*. **11**, 1166 (1994); J.J. McClelland: *ibid*. **12**, 1761 (1995)
10. C.S. Adams, E. Riis: Prog. Quantum Electron. **21**, 1 (1997)
11. Z.T. Lu, K.L. Corwin, M.J. Renn, M.H. Anderson, E.A. Cornell, C. Wieman: Phys. Rev. Lett. **77**, 3331 (1996)
12. W.R. Anderson, C.C. Bradley, J.J. McClelland, R.J. Celotta: Phys. Rev. A **59**, 2476 (1999)
13. C. Salomon, J. Dalibard, A. Aspect, H. Metcalf, C. Cohen-Tannoudji: Phys. Rev. Lett. **59**, 1659 (1987)
14. K.S. Johnson, J.H. Thywissen, N.H. Dekker, K.K. Berggren, A.P. Chu, R. Younkin, M. Prentiss: Science **280**, 1583 (1998)
15. J. Chen, J.G. Story, J.J. Tollett, R.G. Hulet: Phys. Rev. Lett. **69**, 1344 (1992)
16. The robustness of the adiabatic focusing serves as an advantage here. For example, if w_y is chosen as the required width of the deposited area, the laser intensity varies by $\sim 40\%$ across the y direction. Still, this variation has very little effect on the focusing properties, as seen below.
17. A. Aspect, J. Dalibard, A. Heidmann, C. Salomon, C. Cohen-Tannoudji: Phys. Rev. Lett. **57**, 1688 (1986)
18. C. Cohen-Tannoudji: *Les Houches, Session LIII, 1990 – Fundamental Systems in Quantum Optics*, ed. by J. Dalibard, J.M. Raimond, J. Zinn-Justin (Elsevier Science Publishers B. V., Amsterdam 1992)
19. We developed an analytic model also for the red-detuned case and indeed obtained larger values for the optimal detunung and smaller compression as compared to the blue-detuned case.
20. It is also possible to work with two different detunings for the adiabatic and coherent lasers. The phase shift between two laser standing-waves can then be compensated by using a small angle between the nearly counterpropagating beams in one of the standing waves.